

Uranium azide photolysis results in C–H bond activation and provides evidence for a terminal uranium nitride

Robert K. Thomson, Thibault Cantat, Brian L. Scott, David E. Morris, Enrique R. Batista* and Jaqueline L. Kiplinger*

Uranium nitride [U≡N]_x is an alternative nuclear fuel that has great potential in the expanding future of nuclear power; however, very little is known about the U≡N functionality. We show, for the first time, that a terminal uranium nitride complex can be generated by photolysis of an azide (U–N=N=N) precursor. The transient U≡N fragment is reactive and undergoes insertion into a ligand C–H bond to generate new N–H and N–C bonds. The mechanism of this unprecedented reaction has been evaluated through computational and spectroscopic studies, which reveal that the photochemical azide activation pathway can be shut down through coordination of the terminal azide ligand to the Lewis acid B(C₆F₅)₃. These studies demonstrate that photochemistry can be a powerful tool for inducing redox transformations for organometallic actinide complexes, and that the terminal uranium nitride fragment is reactive, cleaving strong C–H bonds.

As we strive to deal with a global energy crisis and anthropogenic global warming, we need to look to alternative energy sources to reduce our dependence on fossil fuels. Nuclear energy provides one possible route to the alleviation of these issues with next-generation nuclear reactors and fuels. In this regard, uranium nitride [U≡N]_x has emerged as a promising alternative to traditional mixed oxide fuels, with advantages such as a higher melting point and enhanced thermal conductivity^{1,2}. Unlike the widely studied uranyl ion [O=U=O]²⁺, very little is known about the U≡N linkage or its chemical behaviour and reactivity^{3–6}. A thorough understanding of the physicochemical properties of the U≡N moiety is critical for predicting the long-term behaviour of the ceramic nuclear fuel [U≡N]_x. The properties of extended ceramic materials are difficult to study, and molecular model systems are therefore ideal for the controlled investigation of this bond fragment. Uranium nitrides are rare, and the few known systems have all been generated through oxidation of reduced uranium centres with either dinitrogen⁷ or azide sources^{8–12}. The nitride fragments in these complexes either form bridging linkages between uranium centres^{7–9,11,12} or coordinate to Lewis acids, namely B(C₆F₅)₃ (ref. 10). These interactions quench any other potential reactivity of the U≡N bond, making the generation of a terminal uranium nitride complex an important goal. The ability to generate a discrete molecular terminal uranium nitride would enable investigation of the fundamental reactivity of the isolated U≡N fragment, which could shed light on the behaviour and properties of bulk [U≡N]_x under life-cycle conditions from fuel-element formulation to recovery and reprocessing.

By far the most effective way in which to access nitride species is through photochemical extrusion of N₂ from metal azide complexes (M–N₃). For example, the photolysis of iron azide complexes has been successfully applied to generate terminal iron nitrides^{13–16}. However, to date, this reaction has not proven successful for analogous uranium complexes. In fact, with the exception of some early reports concerning the photoinduced generation of low-valent

thorium and uranium complexes through β-hydride elimination^{17,18}, the photochemistry of organometallic actinide complexes has remained essentially unexplored. Herein, we demonstrate that a terminal uranium nitride can be generated by photolysis of an azide precursor, and that the U≡N linkage is nucleophilic, activating a C–H bond to form new C–N and N–H bonds. This is the first uranium nitride to be accessed through photolysis. Most importantly, this result demonstrates that the U≡N fragment is not inert and can undergo reactions with strong bonds, with the observed C–H bond addition to the U≡N moiety being strikingly similar to the oxidation of alkanes to alcohols by the cytochrome P450 family of enzymes¹⁹. It is anticipated that these first reactivity studies will open new avenues in the study of U≡N bonds and provide important insights into the generation and reprocessing of [U≡N]_x. Additionally, these results demonstrate the utility of photochemistry for promoting redox processes for organometallic actinides.

Results and discussion

Recently, we reported that (Ph₃P)Au–N₃ is an ideal mild oxidant for the generation of U^{IV} azide complexes from U^{III} precursors²⁰. The solid-state structural parameters of the azide functionality in the aryloxy complex (C₅Me₅)₂U(O–2,6-ⁱPr₂C₆H₃)(N₃) (**1**) were consistent with a typical U–N=N=N bonding description^{20,21}. Photolysis studies of **1** were undertaken, and although these indicated that the azide complex was consumed, the reaction led to the formation of numerous unidentified products. The U^{IV} amide–azide complexes (C₅Me₅)₂U(NPh₂)(N₃) (**2**), (C₅Me₅)₂U[N(SiMe₃)₂](N₃) (**3**) and (C₅Me₄Et)₂U[N(SiMe₃)₂](N₃) (**4**) were also prepared by oxidation of the corresponding U^{III} precursors with (Ph₃P)Au–N₃ (for their solid-state molecular structures, see Fig. 1).

In contrast to the aryloxy–azide complex **1**, the arylamide–azide complex **2** presents a more localized azide fragment with a N(1)–N(2) bond length of 1.20(2) Å, and a N(2)–N(3) bond length of 1.11(2) Å, consistent with a more polarized bonding description that is shifted towards a U=N–N≡N form²¹. These

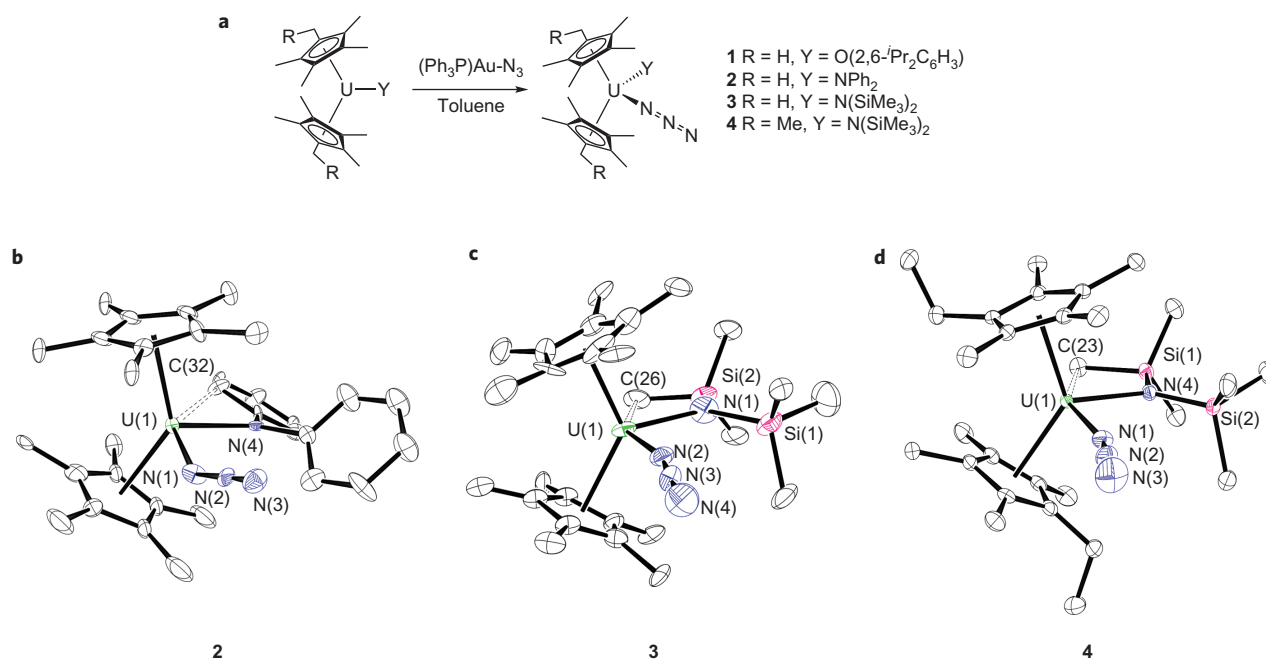


Figure 1 | Generation of U^{IV} azide complexes. **a**, Uranium azide complexes **1–4** were obtained through one-electron oxidation of the corresponding U^{III} precursors with (Ph₃P)Au-N₃. **b–d**, Solid-state structures of **2**, **3** and **4** as determined by single-crystal X-ray diffraction, depicted with 50% probability ellipsoids (hydrogen atoms have been omitted for clarity). Selected bond lengths (Å) and angles (deg) for **2**: U(1)–N(1) = 2.289(15), U(1)–N(4) = 2.325(4), N(1)–N(2) = 1.20(2), N(2)–N(3) = 1.11(2), U(1)–C(32) = 3.356, N(1)–U(1)–N(4) = 97.9(4), U(1)–N(1)–N(2) = 146.2(14), N(1)–N(2)–N(3) = 176.6(19). Selected bond lengths (Å) and angles (deg) for **3**: U(1)–N(1) = 2.21(2), U(1)–N(2) = 2.26(2), N(2)–N(3) = 1.20(3), N(3)–N(4) = 1.14(3), U(1)–C(26) = 3.209, N(1)–U(1)–N(2) = 88.0(7), U(1)–N(2)–N(3) = 163.5(17), N(2)–N(3)–N(4) = 176(3). Selected bond lengths (Å) and angles (deg) for **4**: U(1)–N(1) = 2.262(2), U(1)–N(4) = 2.286(2), N(1)–N(2) = 1.200(3), N(2)–N(3) = 1.145(4), U(1)–C(23) = 3.309, N(4)–U(1)–N(1) = 91.85(8), U(1)–N(1)–N(2) = 160.1(2), N(1)–N(2)–N(3) = 179.3(3).

parameters suggest that photolysis of **2** might lead to elimination of N₂, but, unfortunately, photolysis of **2** also leads to decomposition. Aromatic amines are known photosensitizers²², and we suspect that this results in the photochemical decomposition of **2** through multiple photochemically induced excitations. Azide complex **3** lacks the problematic aryl groups present in complexes **1** and **2** and is cleanly converted to a single product **5** upon photolysis, as illustrated in Fig. 2a.

The formulation of **5** as the mixed-amide complex (C₅Me₅)(C₅Me₄CH₂NH)U[N(SiMe₃)₂] is supported by ¹H nuclear magnetic resonance (NMR) spectroscopy. A single resonance corresponding to the C₅Me₅ protons is present at δ = 1.19, and the freely rotating SiMe₃ group appears at δ = –8.61. The most diagnostic resonances are those for the methylene protons, which appear as diastereotopic doublets at δ = 41.36 and 52.36, and the amide N–H proton, which is present at δ = –111.63, consistent with other complexes bearing U–NHR linkages^{23,24}. Conversion of the azide to an NHR[–] functional group is also corroborated by infrared (IR) spectroscopy, showing that the characteristic strong azide stretch for **3** at 2,090 cm^{–1} is replaced by a weak N–H stretch at 3,308 cm^{–1} for **5**. Figure 2c displays the molecular structure of the photolysis product **5**, which confirms the activation of a C–H bond of the C₅Me₅ ligand to form new N–C and N–H bonds. The U(1)–N(2) bond length of 2.192(3) Å in **5** is consistent with other U^{IV} amide bond lengths^{25–27}. The newly formed metallacycle also features a U(1)–N(2)–C(8) bond angle of 110.6(2)°. The U...H–C agostic interaction observed between the SiMe₃ methyl group (C(26)) and the uranium centre of **3** (U(1)–C(26) = ~3.21 Å) is maintained in the photolysis product **5**, where a close contact of ~3.21 Å exists between C(22) and U(1) in the solid state. This agostic interaction is also present in solution, as determined by ¹H NMR spectroscopy, there being seven distinct singlet resonances corresponding to the four

inequivalent methyl groups on the C₅Me₅ ligand involved in the C–H activation reaction, and the three methyl groups of the SiMe₃ group involved in the agostic interaction. These signals appear at δ = –27.08, –2.57, 1.04, 1.19, 11.49, 17.18 and 23.06, and integrate to three protons each.

As suggested in Fig. 2a, the conversion of **3** to **5** is proposed to proceed through initial loss of N₂ to generate a terminal uranium nitride, followed by C–H activation. Azide complexes are known precursors for transition metal nitride species, where N₂ loss can be induced through photochemical or redox processes^{13–16}. To the best of our knowledge, the observed subsequent addition of a C–H bond to the nitride fragment in a 1,1-fashion is a previously unknown process for *d*- and *f*-elements. However, this reaction is reminiscent of the oxidation of alkanes by cytochrome P450, resulting in the formation of alcohols (see below)¹⁹. The 1,3-addition of a C–H bond of a C₅Me₅ ligand across a N=U=N π-system has been observed upon thermolysis of the *bis*(imido) system (C₅Me₅)₂U(=NAd)₂ (Ad = 1-adamantyl), resulting in the formation of (C₅Me₅)(C₅Me₄CH₂NAd)U(NHAd), in which the methylene group is bound to one nitrogen and the transferred hydrogen is bound to the other nitrogen²⁵.

In an attempt to trap the putative nitride intermediate, photolysis was performed in the presence of Lewis acids. Photolysis of a 1:1 mixture of (C₅Me₅)₂U[N(SiMe₃)₂](N₃) (**3**) and the weak Lewis acid BPh₃ gave quantitative formation of (C₅Me₅)(C₅Me₄CH₂NH)U[N(SiMe₃)₂] (**5**), showing no reaction with BPh₃. Furthermore, ¹H NMR spectroscopy shows that there is no interaction between **3** and 1 equiv. of BPh₃ at room temperature. In contrast, the stronger Lewis acid B(C₆F₅)₃ forms the stable borane adducts (C₅Me₅)₂U[N(SiMe₃)₂](μ-η¹:η¹-N₃)[B(C₆F₅)₃] (**6**) and (C₅Me₄Et)₂U[N(SiMe₃)₂](μ-η¹:η¹-N₃)[B(C₆F₅)₃] (**7**) upon reaction with azide complexes **3** and **4**, respectively. In

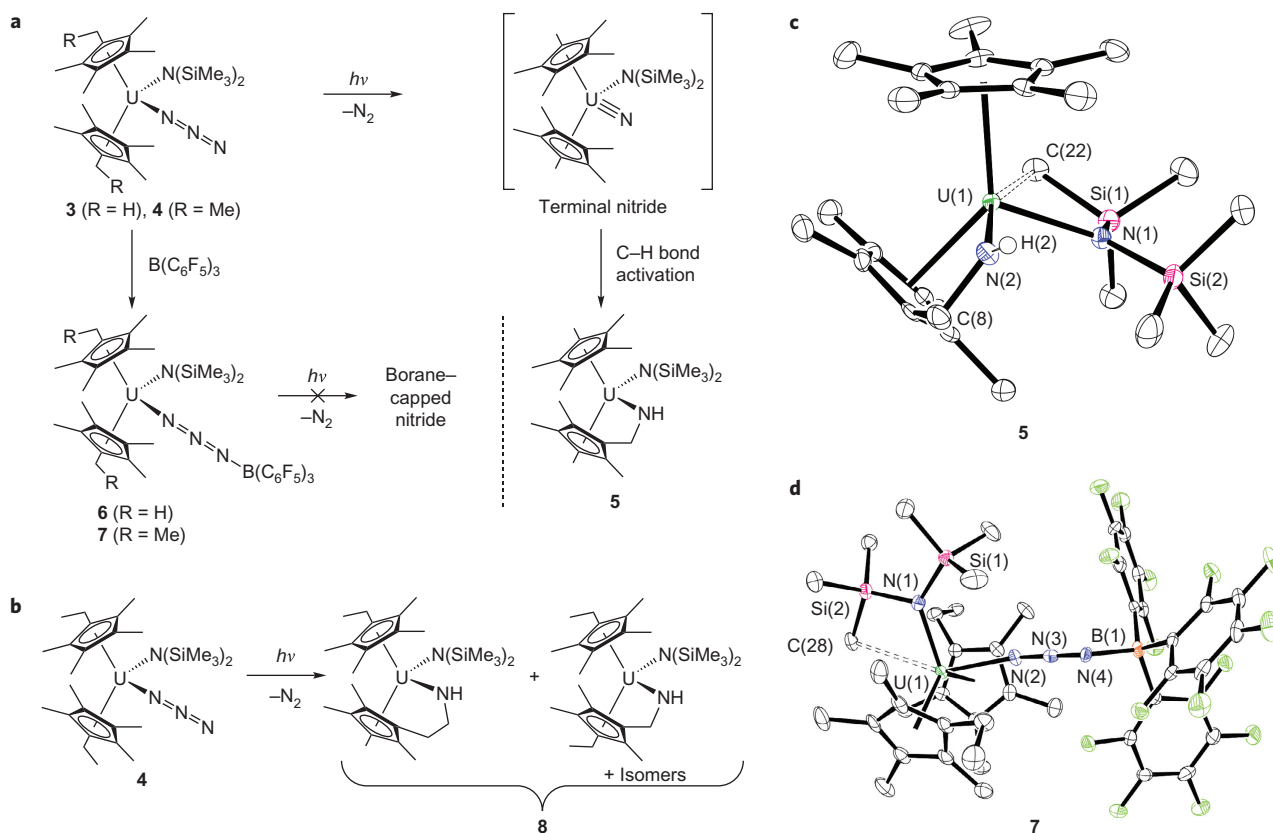


Figure 2 | Photochemical generation and reactivity of terminal uranium nitride. **a**, Photolysis of azide complex **3** generates a transient terminal uranium nitride. C–H bond activation of the C_5Me_5 ligand leads to the formation of **5**. Addition of $B(C_6F_5)_3$ to azide complexes **3** and **4** leads to the formation of azidoborate complexes **6** and **7**, which are deactivated towards photolysis. **b**, Products from photolysis of azide complex **4**. **c**, Solid-state structure of photolysis product **5** as determined by single-crystal X-ray diffraction, with 50% probability ellipsoids. Hydrogen atoms have been omitted for clarity. Selected bond lengths (Å) and angles (deg): U(1)–N(1) = 2.323(3), U(1)–N(2) = 2.192(3), N(2)–C(8) = 1.473(5), U(1)–C(22) = 3.205, N(1)–U(1)–N(2) = 99.72(11), U(1)–N(2)–C(8) = 110.6(2). **d**, Solid-state structure of azidoborate complex **7** as determined by single-crystal X-ray diffraction, with 50% probability ellipsoids. Hydrogen atoms have been omitted for clarity. Selected bond lengths (Å) and angles (deg): U(1)–N(1) = 2.236(3), U(1)–N(2) = 2.424(3), N(2)–N(3) = 1.166(4), N(3)–N(4) = 1.186(4), N(4)–B(1) = 1.605(5), U(1)–C(28) = 3.078, N(1)–U(1)–N(2) = 88.57(10), U(1)–N(2)–N(3) = 170.8(3), N(2)–N(3)–N(4) = 173.9(4), N(3)–N(4)–B(1) = 127.8(3).

solution, 1H NMR spectroscopic data clearly show the formation of the borane adduct by a shift in the C_5Me_5 resonance from $\delta = 8.66$ in **3** to $\delta = 10.18$ in **6**. Likewise, the resonance for the agostic methyl group is shifted from $\delta = -101.60$ in **3** to $\delta = -116.22$ in **6**, and the

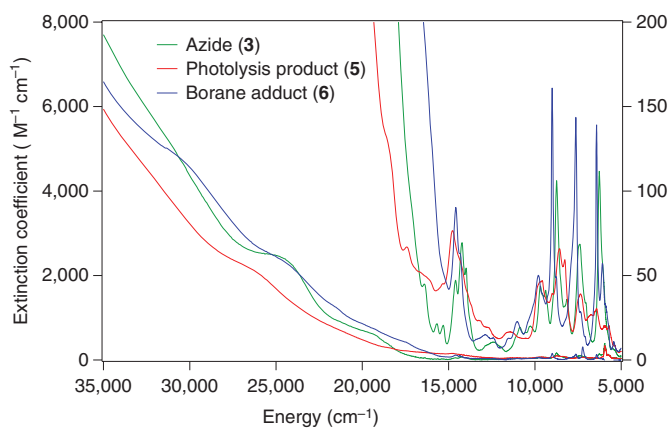


Figure 3 | UV-visible-NIR absorption spectra in a toluene solution. Spectra are shown for the azide complex $(C_5Me_5)_2U[N(SiMe_3)_2](N_3)$ (**3**; green), the photolysis product $(C_5Me_5)(C_5Me_4CH_2NH)U[N(SiMe_3)_2]$ (**5**; red) and the azidoborate complex $(C_5Me_5)_2U[N(SiMe_3)_2](\mu-\eta^1-\eta^1-N_3)[B(C_6F_5)_3]$ (**6**; blue).

$SiMe_2$ and $SiMe_3$ resonances are shifted from $\delta = 3.31$ and 4.79 in **3**, respectively, to $\delta = 6.66$ and 7.08 in **6**. Additional evidence comes from IR spectroscopy, which shows that the diagnostic asymmetric azide stretch is shifted from $2,090\text{ cm}^{-1}$ in complex **3** to $2,178\text{ cm}^{-1}$ in borane adduct **6**. The formation of an azidoborate adduct was confirmed by X-ray crystallography, and the molecular structure of $(C_5Me_4Et)_2U[N(SiMe_3)_2](\mu-\eta^1-\eta^1-N_3)[B(C_6F_5)_3]$ (**7**) is given in Fig. 2d. The coordination of the borane weakens the uranium azide linkage, as indicated by a profound elongation of the U(1)–N_{azide} bond length from $2.262(2)\text{ Å}$ in **4** to $2.424(3)\text{ Å}$ in **7**. The N(4)–B(1) bond length of $1.605(5)\text{ Å}$ is similar to that reported for the azidoborate salt $[Me_4N][N_3B(C_6F_5)_3]$ (N–B = $1.584(4)\text{ Å}$)²⁸, which is consistent with a dative N → B bond. The borane adducts are easily disrupted by other donors, and upon dissolution in tetrahydrofuran (THF) adducts **6** and **7** are converted to the terminal azides **3** and **4**, respectively. Photolysis of **6** and **7** in non-coordinating solvents results in no reaction, indicating that coordination of the azide ligand to the boron centre deactivates the azide group towards N_2 loss.

As seen from the UV-visible-NIR spectral data in Fig. 3, the azide complex **3** and borane adduct **6** are both $5f^2 U^{IV}$ complexes with grossly similar spectral properties. The photolysis product **5** shows markedly different spectral behaviour due to the absence of the azide ligand. In the NIR region, coordination of the borane results in a wholesale shift of the $f-f$ ligand-field transitions to

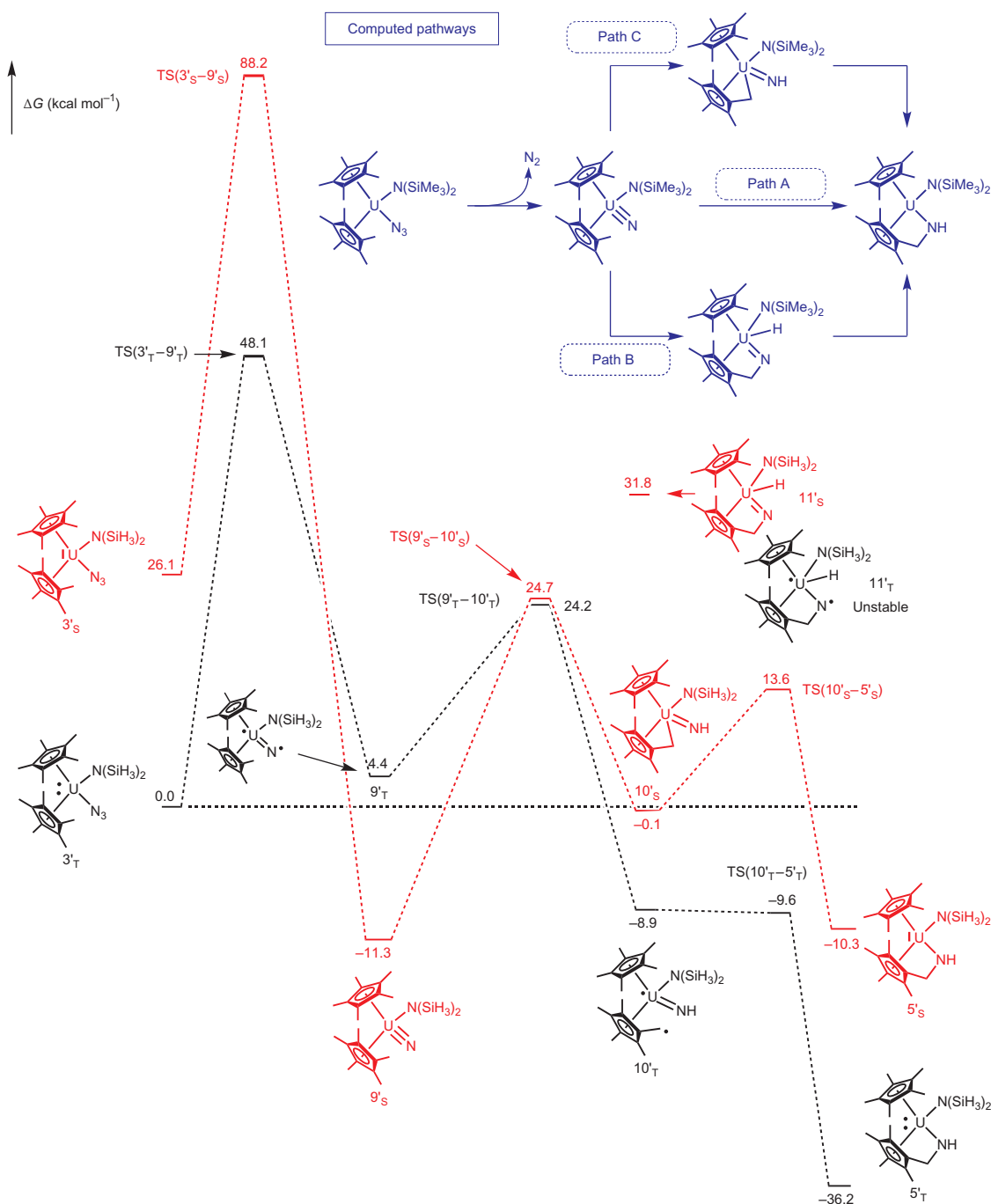


Figure 4 | DFT calculations on the mechanism for the formation of **5** from **3**. Calculated relative energies (kcal mol^{-1}) of the azide precursor ($\text{C}_5\text{Me}_5)_2\text{U}[\text{N}(\text{SiH}_3)_2](\text{N}_3)$ (**3'**), nitride ($\text{C}_5\text{Me}_5)_2(\text{U}=\text{N})[\text{N}(\text{SiH}_3)_2]$ (**9'**) and imido-tuck-in ($\text{C}_5\text{Me}_5)(\text{C}_5\text{Me}_4\text{CH}_2)(\text{U}=\text{NH})[\text{N}(\text{SiH}_3)_2]$ (**10'**) intermediates, and photolysis product ($\text{C}_5\text{Me}_5)(\text{C}_5\text{Me}_4\text{CH}_2\text{NH})\text{U}[\text{N}(\text{SiH}_3)_2]$ (**5'**). Imido-hydride intermediates ($\text{C}_5\text{Me}_5)(\text{C}_5\text{Me}_4\text{CH}_2\text{N})(\text{U}-\text{H})[\text{N}(\text{SiH}_3)_2]$ (**11'**) from the 1,2-addition pathway are given for comparison. Transition states are labeled 'TS'. Red structures represent the singlet (**S**) spin state and black structures the triplet (**T**) spin state. Calculations were performed on model systems using SiH_3 substituents in place of SiMe_3 ; this simplification has no significant impact on the energetics of the pathways. (For full details regarding the simplification from SiMe_3 to SiH_3 , see Supplementary Information.)

higher energy ($250\text{--}350\text{ cm}^{-1}$), indicating that the distal borane is perturbing the ligand field at the U^{IV} ion.

Density functional theory (DFT) calculations were performed to gain insight into the chemical properties of the $\text{U}=\text{N}$ linkage, as they afford a model to explain the role of photochemistry in promoting the activation of the azide complex **3** and to propose a viable mechanism for the C–H activation process. Under photolytic conditions, both singlet and triplet configurations are available for uranium complexes, and the two potential energy

surfaces were computationally explored. As depicted in Fig. 4, the formation of ($\text{C}_5\text{Me}_5)(\text{C}_5\text{Me}_4\text{CH}_2\text{NH})\text{U}[\text{N}(\text{SiH}_3)_2]$ (**5'**) from the starting azide complex ($\text{C}_5\text{Me}_5)_2\text{U}[\text{N}(\text{SiH}_3)_2](\text{N}_3)$ (**3'**) is an exergonic process for both spin states, with an overall release in free energy of $36.2\text{ kcal mol}^{-1}$. This large stabilization is consistent with a process releasing N_2 together with the formation of strong N–H and C–H bonds, and accounts for the quantitative nature of the reaction. The formation of the intermediate nitride complex ($\text{C}_5\text{Me}_5)_2(\text{U}=\text{N})[\text{N}(\text{SiH}_3)_2]$ (**9'**) is slightly endergonic on the

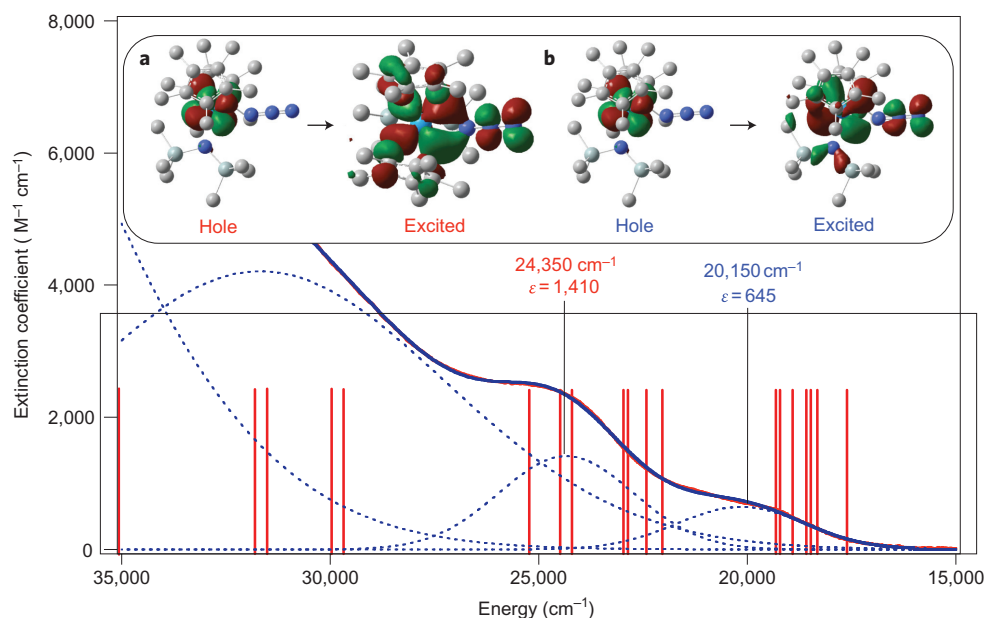


Figure 5 | Deconvoluted UV-vis spectrum of $(C_5Me_5)_2U[N(SiMe_3)_2](N_3)$ (3**) and calculated (TD-DFT) electronic transitions (vertical red lines).** Excellent agreement exists between the clusters of transitions and the positions of spectral features in the UV-vis spectrum. The MLCT band at $24,350\text{ cm}^{-1}$ is reproduced well from calculations. The excited-state orbital representations are given in the inset. **a**, Natural transition orbital of the excited electron (right) arising from the $U(5f) \rightarrow \pi^*$ transition and the hole state (left) (derived from a TD-DFT study; $\sim 25,500\text{ cm}^{-1}$). The metal-based component of the excited electron orbital has a $6d$ character (N, dark blue; U, light blue; C, Si, grey). **b**, Natural transition orbital of the excited electron (right) arising from the $U(5f) \rightarrow \pi^*$ transition and the hole state (left) (derived from a TD-DFT study; $\sim 17,500\text{ cm}^{-1}$). The metal-based component of the excited electron orbital has a $6d$ character. No electron density is present at the uranium-bound N atom of the azide ligand. The electron density is localized between the N atoms of the terminal N_2 fragment of the azide ligand (N, dark blue; U, light blue; C, Si, grey).

triplet surface ($\Delta G = 4.4\text{ kcal mol}^{-1}$), but is exergonic for the singlet system ($\Delta G = -11.3\text{ kcal mol}^{-1}$), with **9'** having a singlet ground-state configuration. Most importantly, N_2 loss from **3'** is a highly energy-intensive process, requiring at least $\sim 48\text{ kcal mol}^{-1}$ for both the triplet and singlet configurations. Such a high energy barrier indicates that this process is not thermally accessible. Indeed, attempts to form **5** from **3** by thermolysis were unsuccessful at temperatures as high as $140\text{ }^\circ\text{C}$.

Because generation of the nitride unit requires an electron transfer from uranium to the azide ligand ($f \rightarrow \pi^*$), leading to N_2 loss, a metal-to-ligand charge transfer (MLCT) has to take place. As determined by UV-visible-NIR spectroscopy, such an electron transfer should occur in the visible region of the spectrum at $\sim 24,300\text{ cm}^{-1}$ (69 kcal mol^{-1}), corresponding to the activation barrier for N_2 loss (Fig. 3). Time-dependent DFT (TD-DFT) calculations of the electronic excited states for the azide complex **3'** describe well the three-peak structure of the experimental UV-vis spectrum (Fig. 5). (For full details of the computational methods, see Supplementary Information.) The lowest calculated excited state ($\sim 17,500\text{ cm}^{-1}$) after the $f \rightarrow f$ manifold contains an MLCT from $U(5f)$ to the azide ligand (π^*). Most importantly, the excited electron orbital has no charge density on the nitrogen proximal to the metal, and all the charge is transferred to the distal N_2 , corroborating the experimentally observed photochemically induced N_2 loss (Fig. 5b). This transition falls under the envelope created by the first peak in the UV-vis spectrum (centred at $20,150\text{ cm}^{-1}$). A similar excited state is also present in the envelope containing the second peak in the UV-vis spectrum (centred at $24,350\text{ cm}^{-1}$); the excited electron orbital is illustrated in Fig. 5a. In this case, the π -electron density is contained within the terminal N_2 unit, but also exhibits a π -bond character between uranium and the adjacent nitrogen, again supporting N_2 extrusion, coupled with the formation of a $U \equiv N$ fragment.

Irradiation in the NIR region only leads to metal-centred $f-f$ transitions, that is, no significant charge redistribution in the

excited states, and thus irradiation in this region is not sufficient to promote thermal activation of the azide. The necessity of UV-vis photolysis was experimentally established by selective irradiation experiments showing that azide decomposition is not observed under strict NIR excitation. The reactive nature of the nitride intermediate $(C_5Me_5)_2(U \equiv N)[N(SiH_3)_2]$ (**9'**) is supported by the low observed selectivity in the thermal C-H activation of the C_5Me_4Et ligand by the nitride generated upon photolysis of the azide complex $(C_5Me_4Et)_2U[N(SiMe_3)_2](N_3)$ (**4**). This reaction produces all possible C-H activation products (**8**) as determined by 1H NMR spectroscopy (Fig. 2b; see Supplementary Information for full details of the photolysis of **4**), with the N-H resonances falling between $\delta = -107$ and -111 , which compares well to that seen for **5** ($\delta = -111.63$). Similarly, the methylene protons appear between $\delta = 41$ and 55 , consistent with that seen for **5** ($\delta = 41.36$ and 52.36).

The observed C-H activation process can follow three different paths, all of which were investigated (Paths A, B and C; Fig. 4): (i) direct 1,1-insertion of the terminal nitride into the C-H bond of the cyclopentadienyl ligand to convert $(C_5Me_5)_2(U \equiv N)[N(SiH_3)_2]$ (**9'**) to $(C_5Me_5)(C_5Me_4CH_2NH)U[N(SiH_3)_2]$ (**5'**) in one step (Path A); (ii) 1,2-addition of the C-H bond across the $U \equiv N$ fragment to form an imido-hydride intermediate $(C_5Me_5)(C_5Me_4CH_2N)(U-H)[N(SiH_3)_2]$ (**11'**), followed by 1,2-migration of the hydride ligand (Path B), and (iii) formal deprotonation/H-abstraction of the C-H bond followed by formation of the C-N bond (Path C). Considering the high-energy excitation required for the production of nitride **9'**, both spin states (singlet and triplet) are accessible and were computed; however, they do not differ significantly in reactivity, so spin interconversion was not studied. Although a pathway involving direct reaction of the C-H bond with the azide ligand cannot be ruled out, there is no precedent for such a reaction; however, there have been examples of N_2 loss from metal azides to generate nitride complexes¹³⁻¹⁶.

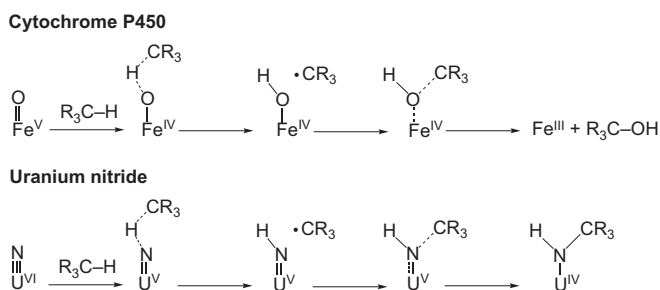


Figure 6 | Analogy between cytochrome P450 and uranium nitride C–H activation. Reaction of the U≡N bond with a C–H bond occurs through the same basic series of steps as the reaction of the Fe=O moiety with C–H bonds in cytochrome P450.

Although the addition of B–C bonds to osmium nitrides in a 1,1-fashion has been observed²⁹, an analogous process involving direct addition of the C–H bond to the U≡N fragment in a 1,1-fashion could not be computationally identified and converged instead to Path C. Addition of the C–H bond to the nitride fragment in a 1,2-fashion was also investigated, but the resulting imido-hydride complexes ($11'_S$, $11'_T$) were too high in energy to be viable ($11'_T$ was found to be unstable, leading to cyclopentadienyl dissociation). The lowest-energy pathway was found to be deprotonation (singlet surface)/H-abstraction (triplet surface) of the methyl group by the nucleophilic nitride unit, which passes through an energetic transition state requiring ~ 20 (triplet)– 36 (singlet) kcal mol⁻¹ to generate an imido tuck-in complex (C_5Me_5)($C_5Me_4CH_2$)(U=NH)[N(SiH₃)₂] ($10'_S$, $10'_T$), with the triplet U^V spin state ($10'_T$) being favoured by 8.8 kcal mol⁻¹. This intermediate is plausible given the large number of uranium tuck-in complexes^{30,31} and high-valent uranium imido complexes that have been reported^{32,33}. In contrast, high-valent uranium hydride species are currently unknown. Subsequent 1,2-migration (singlet surface)/radical recombination (triplet surface) of the methylene group from the uranium centre to nitrogen requires ~ 14 kcal mol⁻¹ on the singlet surface and essentially no energy on the triplet surface to traverse the transition state, with the final product $5'_T$ lying 36.2 kcal mol⁻¹ below the azide starting material $3'_T$, and 24.9 kcal mol⁻¹ below the singlet nitride complex ($9'_S$). This mechanism is reminiscent of that proposed for the cytochrome P450 family of enzymes, which oxidize C–H bonds to alcohols (R–OH functionality) through formal 1,1-insertion of an iron-oxo (Fe=O) complex into a C–H bond¹⁹. By direct analogy, here we see that the uranium nitride (U≡N) inserts into a C–H bond in a 1,1-fashion (Fig. 6).

In summary, we have shown that photolysis of a uranium azide complex can promote the release of N₂ to generate a terminal uranium nitride. The U≡N fragment in this complex is nucleophilic and engages in C–H bond activation, proceeding through initial deprotonation of the C–H bond, followed by U–C bond migration to the incipient U=NH moiety. This unprecedented transformation illustrates that photochemistry can serve as a powerful tool for promoting new redox processes with organometallic uranium species, and may lead to the discovery of new photochemical reaction pathways for the actinides.

Methods

Preparation of (C_5Me_5)₂U[N(SiMe₃)₂](N₃), 3. The syntheses of azide complexes 1–4 are completely analogous, and the preparation of 3 is given as a representative example. A 125-ml side-arm flask equipped with a stir bar was charged with (C_5Me_5)₂U[N(SiMe₃)₂] (0.875 g, 1.31 mmol) and toluene (50 ml). To this green solution was added (Ph₃P)Au–N₃ (0.656 g, 1.31 mmol). The solution immediately turned dark red in colour and was stirred at room temperature. After 15 h, the solution was filtered through a Celite-padded coarse-porosity fritted filter and the Celite plug was washed with toluene (10 ml) until the washings were colourless. The

filtrate was collected and volatiles were removed under reduced pressure to give a red residue, which was dissolved in hexanes (30 ml) and filtered through a Celite-padded coarse-porosity fritted filter. The Celite plug was washed with hexane (10 ml) until the washings were colourless. The resulting red filtrate was collected and volatiles were removed under reduced pressure to give 3 as dark red crystals (0.825 g, 1.17 mmol, 89% yield). ¹H NMR (300 MHz, benzene-*d*₆, 25 °C): $\delta = -101.60$ (s, 3H, SiCH₃), 3.31 (s, 6H, Si(CH₃)₂), 4.79 (s, 9H, Si(CH₃)₃), 8.66 (s, 30H, C₅Me₅). Infrared (Nujol, cm⁻¹): ν 2,090(s) (N₃ asymmetric stretch). MS (EI, 70 eV): m/z 710 [M⁺]. Analysis. Found: C, 44.22; H, 6.69; N, 7.87. C₂₆H₄₈N₄Si₂U requires C, 43.93; H, 6.81; N, 7.88.

Preparation of (C_5Me_5)($C_5Me_4CH_2NH$)U[N(SiMe₃)₂], 5. A 20-ml thick-walled Schlenk tube equipped with a Teflon valve and a stir bar was charged with (C_5Me_5)₂U[N(SiMe₃)₂](N₃) (3) (0.250 g, 0.352 mmol) and toluene (15 ml). The Teflon valve was wrapped with aluminium foil to prevent degradation. The reaction vessel was irradiated at room temperature using a water-cooled Hanovia 450 W medium-pressure Hg lamp filtered through a Pyrex cell at a distance of ~ 5 cm. After 80 h, the volatiles were removed from the reaction mixture under reduced pressure to yield a red-brown solid, which was dissolved in hexane (20 ml) and filtered through a Celite-padded coarse-porosity fritted filter. The filtrate was washed with hexane (5 ml) until the washings became colourless. The filtrate was collected and the volatiles were removed under reduced pressure to give 5 as a red-brown solid (0.200 g, 0.299 mmol, 85% yield). X-ray-quality crystals of 5 were obtained from saturated hexane or toluene solutions at -30 °C. ¹H NMR (300 MHz, benzene-*d*₆, 25 °C): $\delta = -111.63$ (s, 1H, NH), -27.08 (s, 3H, CH₃), -8.61 (s, 9H, Si(CH₃)₃), -2.57 (s, 3H, CH₃), 1.04 (s, 3H, CH₃), 1.19 (s, 18H, C₅Me₅ + CH₃), 11.49 (s, 3H, CH₃), 17.18 (s, 3H, CH₃), 23.06 (s, 3H, CH₃), 41.36 (d, $J = 11$ Hz, 1H, CH₂), 52.36 (d, $J = 11$ Hz, 1H, CH₂). Infrared (Nujol, cm⁻¹): ν 3,308(w) (NH stretch). MS (EI, 70 eV): m/z 682 [M⁺]. Analysis. Found: C, 45.17; H, 7.03; N, 4.32. C₂₆H₄₈N₂Si₂U requires C, 45.73; H, 7.08; N, 4.10.

Preparation of (C_5Me_4Et)₂U[N(SiMe₃)₂](μ - η^1 - η^1 -N₃)[B(C₆F₅)₃], 7. The syntheses of azidoborate complexes 6 and 7 are completely analogous, and the preparation of 7 is given as a representative example. A 20-ml scintillation vial equipped with a stir bar was charged with (C_5Me_4Et)₂U[N(SiMe₃)₂](N₃)(4) (0.100 g, 0.135 mmol) and toluene-*d*₆ (3 ml). To this red solution was added B(C₆F₅)₃ (0.069 g, 0.135 mmol). The solution immediately became dark red in colour and was stirred at room temperature. After 15 h, the solution was filtered through a Celite-padded coarse-porosity fritted filter and the Celite plug was washed with benzene (5 ml) until the washings were colourless. The filtrate was collected and volatiles were removed under reduced pressure to give a red residue, which was triturated with pentane (20 ml) and collected on a medium-porosity fritted filter (0.100 g). The resulting red filtrate was collected and volatiles were removed under reduced pressure to yield a dark red solid (0.035 g). ¹H NMR spectroscopy confirmed that both products were 7 (0.135 g, 0.108 mmol, 80% yield). Single crystals for X-ray diffraction were grown from a saturated solution of (Me₃Si)₂O with minimal THF at -30 °C. ¹H NMR (300 MHz, toluene-*d*₆, 25 °C): $\delta = -116.40$ (s, 3H, Si(CH₃)₃), -0.51 (m, 2H, C₅Me₄CH₂CH₃), 0.78 (m, 2H, C₅Me₄CH₂CH₃), 6.45 (s, 6H, Si(CH₃)₂), 6.84 (s, 9H, Si(CH₃)₃), 7.07 (t, $J = 7$ Hz, 6H, C₅Me₄CH₂CH₃), 9.04 (s, 6H, C₅Me₄Et), 10.47 (s, 6H, C₅Me₄Et), 10.63 (s, 6H, C₅Me₄Et), 12.35 (s, 6H, C₅Me₄Et). ¹⁹F NMR (282 MHz, toluene-*d*₆, 25 °C): $\delta = -147.92$ (d, $J = 20$ Hz, 6F, *o*-Ar-F), -160.30 (t, $J = 20$ Hz, 3F, *p*-Ar-F), -168.12 (m, 6F, *m*-Ar-F). Infrared (Nujol, cm⁻¹): ν 2,180(s) (N₃ asymmetric stretch). Analysis. Found: C, 43.93; H, 4.14; N, 4.24. C₄₆H₅₂BF₁₅N₄Si₂U requires C, 44.17; H, 4.19; N, 4.48.

Received 5 February 2010; accepted 17 May 2010;
published online 11 July 2010

References

- Yeaman, C. B. *et al.* Oxidative ammonolysis of uranium(IV) fluorides to uranium(VI) nitride. *J. Nucl. Mater.* **374**, 75–78 (2008).
- Streit, M. & Ingold, F. Nitrides as a nuclear fuel option. *J. Eur. Ceram. Soc.* **25**, 2687–2692 (2005).
- Denning, R. G. Electronic structure and bonding in actinyl ions and their analogs. *J. Phys. Chem. A* **111**, 4125–4143 (2007).
- Arnold, P. L. *et al.* Reduction and selective oxo group silylation of the uranyl dication. *Nature* **451**, 315–317 (2008).
- Burdet, F., Pecaut, J. & Mazzanti, M. Isolation of a tetrameric cation–cation complex of pentavalent uranyl. *J. Am. Chem. Soc.* **128**, 16512–16513 (2006).
- Steele, H. & Taylor, R. J. A theoretical study of the inner-sphere disproportionation reaction mechanism of the pentavalent actinyl ions. *Inorg. Chem.* **46**, 6311–6318 (2007).
- Korobkov, I., Gambarotta, S. & Yap, G. P. A. A highly reactive uranium complex supported by the calix[4]tetrapyrrole tetraanion affording dinitrogen cleavage, solvent deoxygenation, and polysilanol depolymerization. *Angew. Chem. Int. Ed.* **41**, 3433–3436 (2002).
- Evans, W. J., Kozimor, S. A. & Ziller, J. W. Molecular octa-uranium rings with alternating nitride and azide bridges. *Science* **309**, 1835–1838 (2005).

- Evans, W. J. *et al.* Analysis of uranium azide and nitride complexes by atmospheric pressure chemical ionization mass spectrometry. *Inorg. Chem.* **46**, 8008–8018 (2007).
- Fox, A. R. & Cummins, C. C. Uranium–nitrogen multiple bonding: the case of a four-coordinate uranium(vi) nitridoborate complex. *J. Am. Chem. Soc.* **131**, 5716–5717 (2009).
- Fox, A. R., Arnold, P. L. & Cummins, C. C. Uranium–nitrogen multiple bonding: isostructural anionic, neutral and cationic uranium nitride complexes featuring a linear U=N=U core. *J. Am. Chem. Soc.* **132**, 3250–3251 (2010).
- Nocton, G., Pecaut, J. & Mazzanti, M. A nitrido-centered uranium azido cluster obtained from a uranium azide. *Angew. Chem. Int. Ed.* **47**, 3040–3042 (2008).
- Berry, J. F. *et al.* An octahedral coordination complex of iron(vi). *Science* **312**, 1937–1941 (2006).
- Vogel, C. *et al.* An iron nitride complex. *Angew. Chem. Int. Ed.* **47**, 2681–2684 (2008).
- Scepaniak, J. J. *et al.* Structural and spectroscopic characterization of an electrophilic iron nitrido complex. *J. Am. Chem. Soc.* **130**, 10515–10517 (2008).
- Scepaniak, J. J. *et al.* Formation of ammonia from an iron nitrido complex. *Angew. Chem. Int. Ed.* **48**, 3158–3160 (2009).
- Kalina, D. G., Marks, T. J. & Wachter, W. A. Photochemical synthesis of low-valent organothorium complexes. Evidence for photoinduced β -hydride elimination. *J. Am. Chem. Soc.* **99**, 3877–3879 (1977).
- Bruno, J. W. *et al.* Mechanistic study of photoinduced β -hydride elimination. The facile photochemical synthesis of low-valent thorium and uranium organometallics. *J. Am. Chem. Soc.* **104**, 1860–1869 (1982).
- Shaik, S. *et al.* Theoretical perspective on the structure and mechanism of cytochrome P450 enzymes. *Chem. Rev.* **105**, 2279–2328 (2005).
- Thomson, R. K. *et al.* Noble reactions for the actinides: safe gold-based access to organouranium and azido complexes. *Eur. J. Inorg. Chem.* 1451–1455 (2009).
- Dori, Z. & Ziolo, R. F. Chemistry of coordinated azides. *Chem. Rev.* **73**, 247–254 (1973).
- Rozsnyai, L. F. & Wrighton, M. S. Selective electrochemical deposition of polyaniline via photopatterning of a monolayer-modified substrate. *J. Am. Chem. Soc.* **116**, 5993–5994 (1994).
- Arney, D. S. J. & Burns, C. J. Synthesis and properties of high-valent organouranium complexes containing terminal organoimido and oxo functional groups. A new class of organo-f-element complexes. *J. Am. Chem. Soc.* **117**, 9448–9460 (1995).
- Peters, R. G., Warner, B. P. & Burns, C. J. The catalytic reduction of azides and hydrazines using high-valent organouranium complexes. *J. Am. Chem. Soc.* **121**, 5585–5586 (1999).
- Peters, R. G. *et al.* C–H bond activation with actinides: the first example of intramolecular ring bite of a pentamethylcyclopentadienyl methyl group. *Organometallics* **18**, 2587–2589 (1999).
- Zi, G. *et al.* Preparation and reactions of base-free bis(1,2,4-tri-tert-butylcyclopentadienyl)uranium oxide, Cp²UO. *Organometallics* **24**, 4251–4264 (2005).
- Monreal, M. J. & Diaconescu, P. L. A weak interaction between iron and uranium in uranium alkyl complexes supported by ferrocene diamide ligands. *Organometallics* **27**, 1702–1706 (2008).
- Fraenk, W. *et al.* Pentafluorophenyl and phenyl substituted azidoborates. *Can. J. Chem.* **80**, 1444–1450 (2002).
- Crevier, T. J. & Mayer, J. M. Insertion of an osmium nitride into boron–carbon bonds. *Angew. Chem. Int. Ed.* **37**, 1891–1893 (1998).
- Evans, W. J. *et al.* A crystallizable f-element tuck-in complex: the tuck-in tuck-over uranium metallocene [(C₅Me₅)U{ μ - η^5 : η^1 -C₅Me₃(CH₂)₂}(μ -H)₂U(C₅Me₅)₂]. *Angew. Chem. Int. Ed.* **47**, 5075–5078 (2008).
- Gardner, B. M. *et al.* A crystallizable dinuclear tuck-in-tuck-over tuck-over dialkyl tren uranium complex and double dearylation of BPh₄[−] to give the BPh₂-functionalized metallocycle [U{N(CH₂CH₂NSiMe₃)₂(CH₂CH₂NSiMe₂CHBPh₂)}(THF)]. *J. Am. Chem. Soc.* **131**, 10388–10389 (2009).
- Arney, D. S. J., Burns, C. J. & Smith, D. C. Synthesis and structure of the first uranium(vi) organometallic complex. *J. Am. Chem. Soc.* **114**, 10068–10069 (1992).
- Hayton, T. W. Metal–ligand multiple bonding in uranium: structure and reactivity. *Dalton Trans.* **39**, 1145–1158 (2010).

Acknowledgements

The authors thank the Los Alamos National Laboratory (LANL) G. T. Seaborg Institute for Transactinium Science for a postdoctoral fellowship to R.K.T., LANL for a Director's postdoctoral fellowship to T.C., and the Division of Chemical Sciences, Office of Basic Energy Science, Heavy Element Chemistry program and the LANL Laboratory Directed Research and Development (LDRD) program for funding. R. M. Chamberlin and D. L. Clark (both LANL) are thanked for helpful discussions.

Author contributions

R.K.T. synthesized and characterized the compounds and wrote the manuscript. B.L.S. collected single-crystal X-ray crystallographic data and solved the structures. T.C. and E.R.B. performed DFT calculations. D.E.M. aided in the analysis and interpretation of UV–vis–NIR spectral data. J.L.K. generated and managed the project and helped write the manuscript.

Additional information

The authors declare no competing financial interests. Supplementary information and chemical compound information accompany this paper at www.nature.com/naturechemistry. Reprints and permission information is available online at <http://npg.nature.com/reprintsandpermissions/>. Correspondence and requests for materials should be addressed to E.R.B. and J.L.K.